

A photo-cross-linkable polymeric binder for silicon anodes in lithium ion batteries†

Cite this: *RSC Advances*, 2013, 3, 12625

Received 16th May 2013,

Accepted 12th June 2013

DOI: 10.1039/c3ra42447b

www.rsc.org/advances

A new photo-cross-linkable poly(acrylic acid) (PAA) polymer functionalized with a photoreactive benzophenone group (PAA-BP) was synthesized and examined as a binder for Si-based anodes. Upon UV irradiation, the PAA-BP binders formed an irreversible cross-linked structure through the formation of a new three-dimensional C–C bond network between the benzophenone moiety and the PAA backbone. The photo-cross-linked PAA-BP binder demonstrated a marginal volume expansion (38%) after full lithiation, compared to conventional binders and this resulted in an improved cycle performance of the Si anode over 100 cycles with a high reversible capacity of ca. 1600 mA h g⁻¹. We attributed this phenomenon to the enhanced mechanical properties of the photo-cross-linked PAA-BP binder, which were evaluated using nanoindentation and swelling measurements.

Introduction

Lithium ion batteries (LIBs) have been in the spotlight as one of the most promising energy storage devices in the era of an energy crisis. The potential uses of LIBs in powering future portable electronics, electrical vehicles and energy utility grids have prompted the development of novel materials and systems to enhance the energy density and cycle life of LIBs.^{1–4} Among these materials, silicon has received more attention recently as a next generation anode material due to its superior theoretical specific

capacity of ca. 4200 mA h g⁻¹, which is an order of magnitude higher than that of conventional graphite anodes.^{5–8} Despite these favorable features, silicon based anodes are still far from commercialization due to significant challenges such as the substantial volume change (ca. 300%) during lithiation–delithiation and the safety issues of lithiated silicon. In particular, the volume change causes high stress and pulverization, and eventually breaks the electrical contact of the electrode, resulting in degradation of the electrode and a limited cycle life.^{9,10} Thus, significant research efforts have endeavored to alleviate the aforementioned challenges, to improve the electrochemical performance of Si-based anode materials.^{11–14} As one representative solution, nanostructured Si anode materials^{15–18} with various morphologies such as nanoparticles,^{19,20} nanotubes,²¹ nanowires²² and thin films²³ have been extensively developed to overcome the problem of volume change, and to improve cycle performance. These nanostructured Si anodes offer potential solutions by providing a smaller absolute volume change, as well as the additional benefit of the short diffusion path of the Li⁺ ion to enhance kinetic behavior.

Although remarkable improvements in the electrochemical performance of Si-based anodes have been achieved, relatively less attention has been paid to the development of the inactive, yet still important component of the battery electrode, such as polymer binders. However, recent studies have demonstrated that a robust polymeric binder plays an important role in controlling the electrochemical performance of batteries by inhibiting the mechanical fracture of Si anodes during cycling.^{24–33} In a seminal example, Yushin and co-workers have recently employed a new type of binder, sodium alginate, a high-modulus natural polysaccharide extracted from brown algae, to yield a remarkably stable battery anode compared with conventional polymeric binders such as poly(vinylidene fluoride) (PVDF), poly(acrylic acid) (PAA), and carboxymethyl cellulose (CMC).²⁹ They proposed that the strong interaction between the carboxylic acid groups of the binder and the hydrolyzed thin surfaces of SiO₂ covering the Si particles prevented the anode from disintegrating. As another approach, Choi and co-workers showed that a thermally cross-linked PAA–CMC binder improved the cycle performance of the Si

^aInterdisciplinary School of Green Energy and KIER-UNIST Advanced Center for Energy, Ulsan National Institute of Science and Technology (UNIST), 100 Banyeon-ri, Eonyang-eup, Ulju-gun, Ulsan 689-798, South Korea. E-mail: ktlee@unist.ac.kr; bskim19@unist.ac.kr

^bSchool of Chemical and Biological Engineering, Seoul National University, 1 Gwanangno, Gwanak-gu, Seoul 151-742, South Korea

^cSchool of Mechanical and Advanced Materials Engineering, Ulsan National Institute of Science and Technology (UNIST), 100 Banyeon-ri, Eonyang-eup, Ulju-gun, Ulsan 689-798, South Korea

^dKorea Institute of Energy Research (KIER), Daejeon 305-343, South Korea

† Electronic supplementary information (ESI) available: FTIR spectra of the PAA-BP binder, XRD pattern and TEM images of the carbon-coated silicon active material and representative load-indentation depth curves of the bare and cross-linked PAA-BP. See DOI: 10.1039/c3ra42447b

‡ These authors contributed equally.

anode due to the improved mechanical properties of the three-dimensionally interconnected network.³² In a separate report, Konno and co-workers also investigated whether that PAA binder could be effective in accommodating the large volume expansion of the SiO-based anode because of the physical and chemical cross-linked structures in the PAA polymer layers.³³ However, even though this PAA binder assists in building a cross-linked structure, the chemical interactions between the carboxylic acid groups are still reversible in their chemical nature due to their susceptibility to environmental changes such as humidity and temperature.³⁴ Thus, a reversible chemical de-cross-linking of PAA binders can occur during the processing of the cell assembly in a practical situation, which in turn leads to the rapid degradation of the Si anodes and an increased cell impedance during cycling. Thus far, however, the majority of efforts on the polymeric binder have been limited to the use of conventional polymers without the introduction of a new functionality onto the polymeric binder. Therefore, we report herein the synthesis of robust PAA polymers which are functionalized with a photo-cross-linkable benzophenone (PAA-BP) as a binder for Si-based anodes and demonstrate the improved cycle performance of the Si anode (marginal capacity fading over 100 cycles with a reversible capacity of *ca.* 1600 mA h g⁻¹) due to the irreversible cross-linked structure of the benzophenone moiety under UV irradiation (Fig. 1). To the best of our knowledge, this is the first report of using a photoreactive polymer as a binder for a Si-based anode in lithium ion batteries.

Experimental

Materials

Poly(acrylic acid) (M_w of 50 000 g mol⁻¹) was purchased from Polysciences, *N,N'*-dimethylformamide (DMF), 4-hydroxybenzophenone, 6-bromo-1-hexanol, *N,N'*-(dimethylamino)pyridine and 1-[3-(dimethylamino)propyl]-3-ethylcarbodiimide methiodide were purchased from Sigma-Aldrich. A carbon coating process was used to provide additional conductivity for the silicon powder.

Synthesis of 4-(6-hydroxyhexyloxy)benzophenone

4-Hydroxybenzophenone (2.01 g, 10 mmol) and K₂CO₃ (2.07 g, 15 mmol) were dissolved in 20 ml of DMF, and the solution was stirred for 30 min at 100 °C. To this solution, 6-bromo-1-hexanol (1.99 g, 11 mmol) in 10 ml of DMF was added dropwise and the final solution mixture was stirred overnight at 100 °C. The mixture was cooled to room temperature and the solvent was evaporated under reduced pressure. Excess water was added to the solution to precipitate a white powder, and the product was dried. The product was recrystallized from ethanol.

Synthesis of PAA substituted with the photo-cross-linkable benzophenone (PAA-BP)

Poly(acrylic acid) (1.0 g, 14 mmol), *N,N'*-(dimethylamino)pyridine (DMAP) (0.34 g, 2.8 mmol) and 4-(6-hydroxyhexyloxy)benzophenone (0.84 g, 2.8 mmol) were dissolved in 50 ml of DMF at 0 °C. 1-[3-(Dimethylamino)propyl]-3-ethylcarbodiimide methiodide (EDC) (1.67 g, 5.6 mmol) was added to the solution. After 30 min, the mixture was warmed to room temperature and stirred overnight.

The mixture was then added dropwise to acetone to form a precipitate. The solid product was washed twice with acetone. The pure product was prepared by dialysis against deionized water adjusted to pH 3, for 3 days to remove any residual byproduct. The degree of substitution was determined to be around 3.7%, on the basis of the ¹H NMR spectrum.

Synthesis of the carbon-coated Si nanoparticles

Si nanopowder (<100 nm, 0.4 g, Aldrich) was mixed with phthalocyanine (0.1 g, Aldrich) using a mortar, and then the mixture was heated at 900 °C for 2 h under Ar. This carbon-coated silicon powder was used as the active material to evaluate the performance of the binders.

Electrochemical characterization

Galvanostatic charge and discharge cycling (WonATech WBCS 3000 battery measurement system) was performed in the potential window from 0.0 to 2.0 V vs. Li/Li⁺ with a two-electrode 2016 coin-type half cell, where Li metal foil was used as the counter electrode. The Si active materials were mixed with carbon black (Super P) and the PAA-BP binder in an 8 : 1 : 2 weight ratio to fabricate the working electrodes. The first lithium insertion and extraction capacities were measured at a current density of 100 mA g⁻¹, and the cycling performance of the half cells was monitored at a current density of 200 mA g⁻¹ at 30 °C. To investigate the rate performance of the half cells, the lithium deinsertion capacities were measured at current densities of 0.2–20 A g⁻¹ at 30 °C. The electrolyte was comprised of 1.3 M LiPF₆ in a mixture of ethylene carbonate (EC) and diethyl carbonate (DEC) (30 : 70, v/v) with 5 wt% fluoroethylene carbonate (FEC, Soulbrain Co. Ltd.). A microporous polyethylene film was used as a separator. The cells were assembled in an Ar-filled glove box with less than 1 ppm of both oxygen and moisture present. After cycling, the cells were carefully opened in a glove box to retrieve their electrodes, and the electrodes were subsequently rinsed in dimethyl carbonate (DMC) to remove the residual LiPF₆-based electrolyte, and dried at room temperature. These dried electrodes were utilized for the *ex situ* measurement of the thickness change.

Photo-cross-linking

The electrodes with the PAA-BP binder were irradiated for 30 min in air by a UV lamp (UVP, 100 W) at a distance of 15 cm. The electrodes were placed at the center of the box having dimensions of 15.5 × 16.5 × 15 cm³. The UV intensity was 391 mW cm⁻².

Nanoindentation test of the bare and cross-linked PAA-BP binders

Nanoindentation experiments were conducted at room temperature using an XP module of a G200 (Agilent, Santa Clara, CA) instrument with a three-sided pyramidal Berkovich indenter. Tests were carried out at a constant indentation strain rate of 0.05 s⁻¹ and the thermal drift was maintained below 0.05 nm s⁻¹. Sixteen tests were conducted for each testing condition, so as to obtain statistically significant data sets. The maximum indentation depths were maintained at 600 nm, which was less than 1/10 of the sample thickness. While the continuous stiffness measurement (CSM) data do not show stable trends at very shallow

indentation depths, due to intrinsic issues in the nanoindentation analysis, the data collected at indentation depths greater than 100 nm show stable trends that are nearly constant for both the hardness and elastic modulus.

Swelling test of the bare and cross-linked PAA-BP binders

A PAA-BP solution was deposited on Si wafers using a spin-coating method. The thickness of every film was measured independently before soaking the film in the diethyl carbonate (DEC) solution and the average thickness was around 20 nm. The PAA-BP films were irradiated for 30 min by a UV lamp. The bare PAA-BP films and cross-linked PAA-BP films were placed in a container filled with the DEC solution. The film thickness was measured at predetermined time points (5, 15, and 30 min) by ellipsometry.

Characterizations

Powder X-Ray diffraction (XRD) data were collected on a Rigaku D/MAX 2500V PC powder diffractometer using Cu-K α radiation ($\lambda = 1.5405 \text{ \AA}$) operated from $2\theta = 10\text{--}80^\circ$. The carbon coating morphology was examined using a field emission transmission electron microscope (TEM; JEOL JEM-2100F) operating at 200 kV. ^1H NMR spectroscopy (VNMRs 600 spectrometer 600 MHz, Varian, USA) was performed with CDCl_3 and $\text{DMSO-}d_6$ as the solvents. The morphology of the electrode was monitored using a field emission scanning electron microscope (SEM; Nano230, FEI, USA). The photo-cross-linking process was investigated by ultraviolet-visible (UV-vis) spectroscopy (Varian, Cary 5000) and Fourier transform infrared (FTIR) spectroscopy (Varian). The change in the thickness of the PAA-BP thin film on the SiO_2 substrates was measured by ellipsometry (EC-400 and M-2000 V, J. A. Woollam Co., Inc.).

Results and discussion

The schematic diagram in Fig. 1 shows our strategy for how the PAA-BP binder can accommodate the huge volume change of the Si anode during lithiation and delithiation. The role of the three-dimensionally interconnected binder structure is to efficiently accommodate the repetitive volume changes upon cycling. Without the cross-linked binders, the composite electrode is gradually deformed on cycling, due to the linear polymeric structure of the binders and finally loses the electrical contact between the electroactive powders.

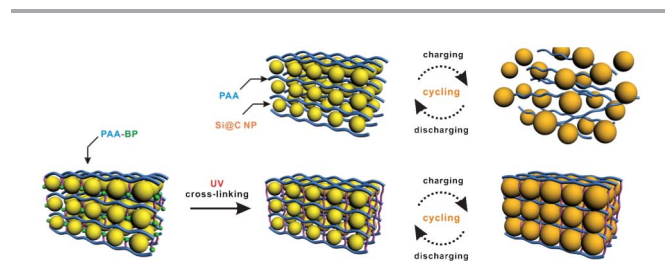


Fig. 1 Schematic illustration of the irreversible cross-linked structure of the PAA-BP binder to accommodate the volume expansion of the Si anode during charging-discharging cycles.

However, the cross-linked structure enables us to limit the deformation of the composite electrode due to the strong irreversible covalent chemical bond formed between the linear polymers. It is known that the PAA binder forms a cross-linked anhydride structure by a dehydration reaction between carboxylic groups at high temperature (150°C), which results in the improvement of the cycle performance due to the effectively suppressed volume expansion of the Si particle.^{32,33} However, this thermal cross-linking of carboxylic acid groups is still reversible and susceptible to environmental changes such as humidity and temperature, as proved by FTIR measurements (Fig. S1, ESI †). Accordingly, the irreversible cross-linking, regardless of environmental changes, is required for the long-term storage of the electrodes under practical conditions. The benzophenone (BP) moiety has been traditionally employed in chemical and industrial applications as a photo-responsive unit.^{35,36} The BP moiety of the PAA-BP polymer provides an irreversible cross-linked structure by the formation of a covalent bond between BP and the backbone of PAA upon UV irradiation, leading to the enhanced mechanical and chemical stabilities that endures environmental changes. More specifically, an excited BP forms a biradical species under UV irradiation ($\lambda_{\text{ex}} = 365 \text{ nm}$) that can abstract hydrogen from the neighboring PAA backbone (C-H) to form a cross-linked structure by a new C-C bond.

In this study, PAA-BP was prepared as shown in Fig. 2(a).³⁵ The successful conjugation of BP along the backbone of PAA was characterized using ^1H NMR spectroscopy with the degree of substitution determined to be around 3.7% (Fig. 2(b)). Although the degree of functionalization can be easily tuned up to 16%, we limited the degree of functionalization to 3.7% in the current study, due to the low solubility of the highly functionalized polymer in water. Polymeric binders should be soluble in solvents such as water and *N*-methyl-2-pyrrolidone (NMP) for the preparation of Si composite electrodes, to obtain a slurry of the active materials. The photo-cross-linking process of PAA-BP is proposed as shown in Fig. 3(a), and this process can be clearly investigated

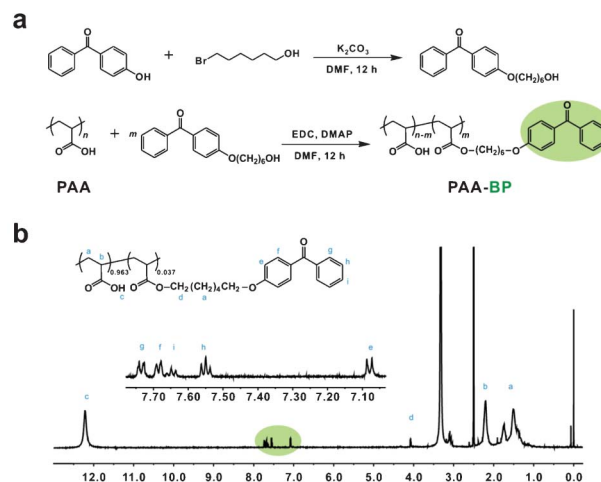


Fig. 2 (a) Synthetic approach for the preparation of the functionalized PAA-BP binder. (b) ^1H NMR spectrum of the PAA-BP in $\text{DMSO-}d_6$ with the corresponding peak assignments. The degree of BP functionalization was calculated to be 3.7%.

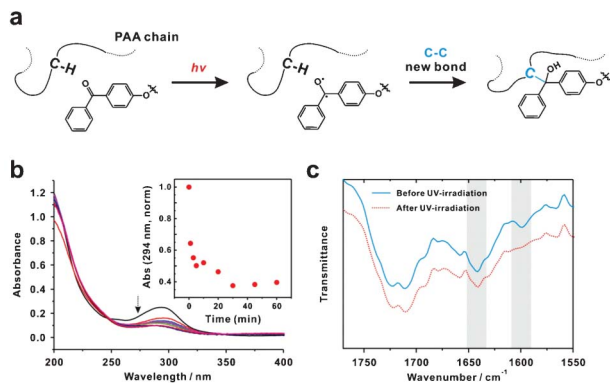


Fig. 3 (a) Proposed mechanism of the cross-linking of the PAA-BP binder. (b) UV-vis spectra of the PAA-BP binder at different UV-irradiation times. Inset: decrease in absorbance of BP moiety at 294 nm upon UV-irradiation. (c) FTIR spectra of the PAA-BP binder (blue solid line) before and (red dotted line) after UV irradiation for 30 min. The characteristic BP peaks at 1600 cm⁻¹ (aromatic ring C=C) and 1641 cm⁻¹ (carbonyl group C=O) decreased upon UV irradiation. For the IR measurements, PAA substituted with 16.7% BP was employed to measure the peaks of PAA-BP clearly.

by UV-vis spectroscopy (Fig. 3(b)). The absorbance of the BP moiety at 294 nm decreased with increased UV irradiation time, due to an increase in the number of n- π^* transitions in the carbonyl group, resulting in the loss of the carbonyl group. To cross check the process of photo-cross-linking in the film state, FTIR spectroscopy measurements were performed (Fig. 3(c)). Before UV irradiation, the characteristic BP peaks at 1600 cm⁻¹ (aromatic ring C=C), 1641 cm⁻¹ (carbonyl group C=O), and the PAA peak at 1710 cm⁻¹ (carboxylic acid group) were observed. Upon UV irradiation, however, the peaks corresponding to the BP moiety significantly decreased, indicating the successful formation of cross-linking.^{35,36}

The electrochemical performance of the carbon-coated Si nanopowder with the PAA-BP binder was evaluated (Fig. 4). Commercial Si nanopowder (<100 nm) was mixed with phthalocyanine and heated at 900 °C for 2 h under an Ar atmosphere to obtain the carbon-coated Si nanopowder (Fig. S2, ESI†).¹⁴ The Si composite electrodes were first prepared with PAA-BP binders, and then the photo-cross-linking reaction of the BP groups was performed *via* the exposure of the electrodes to UV irradiation. As expected, the cross-linked PAA-BP electrode *via* UV irradiation shows a significantly improved capacity retention over 100 cycles, while a gradual capacity fading was observed in the case of the bare PAA-BP binder electrode without UV irradiation (Fig. 4(a)). Their corresponding voltage profiles are presented in Fig. 4(b) and (c), respectively. Moreover, the cross-linked PAA-BP electrode shows a better rate performance than the bare PAA-BP electrode, showing that *ca.* 1420 mA h g⁻¹ is delivered even at a specific current density of 20 A g⁻¹ (*ca.* 12.5 C-rate) (Fig. 4(d)). This improvement in cycle stability and rate performance, realized through UV irradiation, is attributed to the three-dimensionally interconnected binder structure, resulting in a lower deformation of the composite electrode on volume change. This interconnected structure allows a sustained electrical contact between the Si and conducting agent of carbon. The low degree of deformation is also

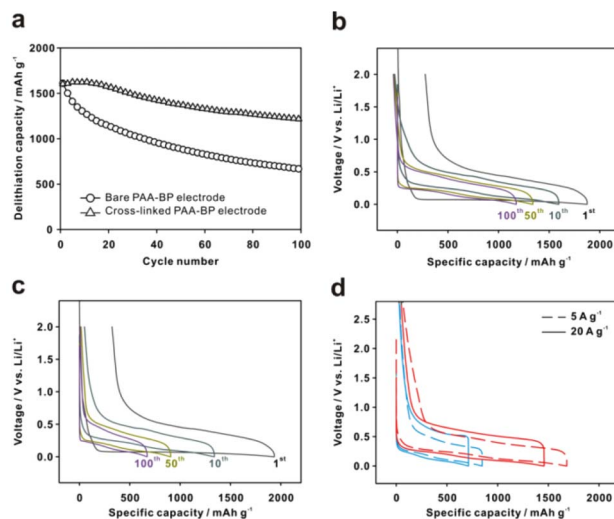


Fig. 4 (a) Cycle performance of (circle) the bare PAA-BP electrode and (triangle) the cross-linked PAA-BP electrode under UV irradiation. Voltage profiles of (b) the cross-linked PAA-BP electrode and (c) the bare PAA-BP electrode at various cycle numbers. (d) Rate performance of (red) the cross-linked and (blue) bare PAA-BP electrodes at different current rates. The electrochemical experiments for the cycle and rate performance were performed in the voltage range 0–2 V and 0–3 V vs. Li/Li⁺, respectively.

supported by the negligible thickness change of the cross-linked PAA-BP electrodes at the first cycle. For that purpose, the thickness change of the electrodes after full lithiation and delithiation was measured *via* an *ex situ* thickness measurement (Fig. 5). The cells were disassembled after cycles of full lithiation–delithiation and the electrode thickness was measured manually. As shown in Fig. 5(a), after full lithiation until the redox potential of the working electrodes reached 0 V vs. Li/Li⁺, the thickness of the cross-linked PAA-BP electrode increased by 38%, whereas the bare PAA-BP electrode expanded by 63%. To our surprise, the thickness of the cross-linked PAA-BP electrode was almost fully recovered to the original state after full delithiation until the redox potential of the working electrodes reached 2 V vs. Li/Li⁺, but the bare PAA-BP electrode remained as the expanded state, even after full delithiation, although the volume expansion decreased from 63 to 38%. In spite of the cross-linked PAA-BP electrode showing a negligible volume change during the first cycle, it was found that the electrode expanded by 230% after 60 cycles. In the case of the bare PAA-BP electrode, however, the electrode was too deformed and eventually detached from the surface of the Cu foil, while the cross-linked PAA-BP electrode was retained conformally on the Cu foil, as shown in the inset of Fig. 5(a). The electrode thickness change of the bare and cross-linked PAA-BP binders was further examined in the cross-sectional SEM images of the electrodes after 60 cycles, as shown in Fig. 5(b) and (c), respectively. It was clearly demonstrated that the bare PAA-BP binder showed a more expanded electrode after cycling, with larger cracks on the surface of the electrode. This feature also indicates that the cross-linked PAA-BP binder exhibited a significantly smaller volume change during cycling, compared to the bare PAA-BP binder, highlighting the improved structural integrity of the cross-linked system.

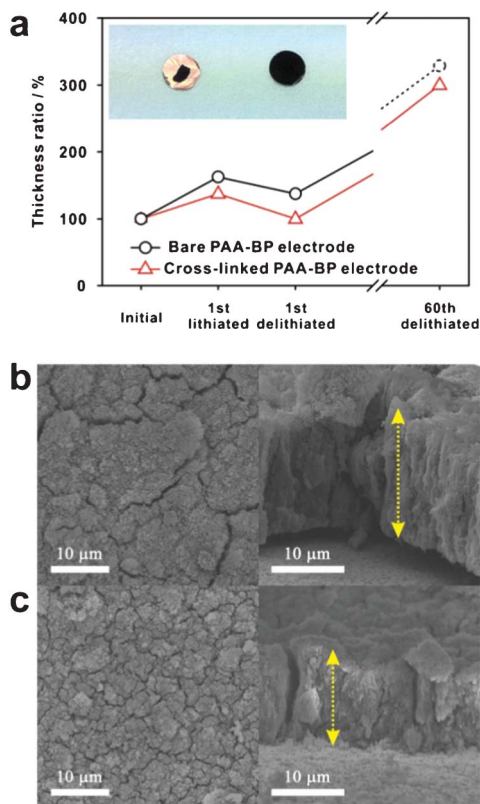


Fig. 5 (a) *Ex situ* measurements for the thickness trace of the PAA-BP electrodes at full lithiation, delithiation and after 60 cycles. Inset image shows the (left) bare and (right) cross-linked electrodes after 60 cycles, indicating disintegration of the bare PAA-BP electrode. The thickness of the bare PAA-BP electrode after 60 cycles was measured with the film residue. Corresponding SEM images of (b) the bare and (c) cross-linked PAA-BP electrodes after 60 cycles. The arrows in the SEM images represent the thickness of the electrode, showing a clear difference between the samples.

However, it is still highly desirable to alleviate the swelling effect for the commercialization of Si-based anodes, although the cross-linked PAA-BP binder efficiently accommodates the volume change of the Si-based electrodes. This work will be the subject of our further research.

Finally, the mechanical properties of the bare and cross-linked PAA-BP binders were evaluated using a nanoindentation method (Fig. 6(a) and (b) and S3, ESI†). The bare PAA-BP electrode showed hardness and elastic modulus values of 0.41 and 6.66 GPa, respectively, at an indentation depth of 100 nm. Upon cross-linking, however, the PAA-BP electrode exhibited significantly enhanced hardness and elastic modulus values of 0.56 and 7.87 GPa, respectively, demonstrating that the effective cross-linking created the interconnected network within the electrode. Also, the observed elastic modulus values are superior to those reported in the case of other conventional polymeric binders such as CMC and alginate (3–5.5 GPa), and PVDF (0.1 to 1.2 GPa).²⁹ In addition, the three-dimensionally interconnected structure of the PAA-BP binders was further confirmed through the wetting behavior of the binder films in the diethyl carbonate (DEC) solution (Fig. 6(c)). The

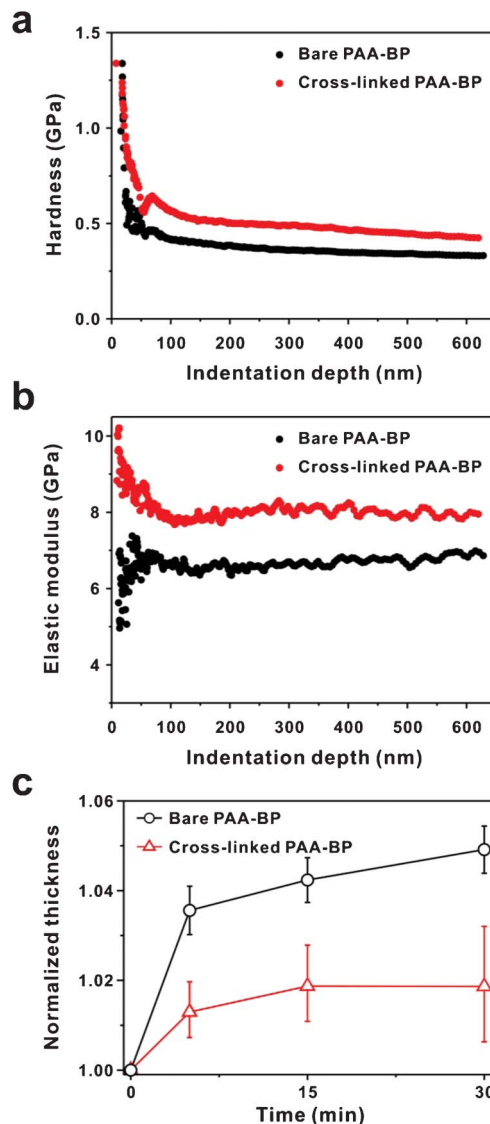


Fig. 6 (a) and (b) Mechanical properties, hardness and elastic modulus of the bare and cross-linked PAA-BP electrodes measured by nanoindentation. (c) Swelling of the bare PAA-BP and cross-linked PAA-BP binders in the DEC solution. The change in the cross-linked PAA-BP binder is lower than for the bare PAA-BP, resulting in stable mechanical properties upon wetting in the aprotic electrolyte solution.

bare PAA-BP and cross-linked PAA-BP polymer films were soaked in the DEC solution, and the thickness change was measured at various soaking times. According to a report by Yushin and co-workers, little, to no interaction between the polymeric binder and the electrolyte is required to achieve stable mechanical properties in the electrolyte. In accordance with that report, our cross-linked PAA-BP binder showed little wetting (101.8%) in the DEC solution, whereas the bare PAA-BP films displayed a relatively larger wetting (104.9%), suggesting a good mechanical stability of the cross-linked binder in the electrolyte solution.²⁹

Conclusions

In conclusion, we have demonstrated that a PAA-BP binder accommodates the volume expansion of a Si-based electrode *via* an irreversible cross-linked structure under UV irradiation. Without UV irradiation, the bare PAA-BP binder shows a significant deformation of the electrode, resulting in an unstable cycle stability. Upon UV irradiation, however, the irreversible cross-linked PAA-BP binder exhibits an improvement in its electrochemical performance with a high reversible capacity of 1600 mA h g⁻¹. We believe that this study on the functionalized polymeric binder will impact on the development of the next generation lithium ion batteries.

Acknowledgements

This work was supported by the WCU (World Class University) program (R31-2008-000-20012-0), Korea Institute of Energy Research (No. GP2012-0024-03), New & Renewable Energy of the Korea Institute of Energy Technology Evaluation and Planning (KETEP) grant funded by the Korea government Ministry of Knowledge Economy (20113020030060), the ITRC (Information Technology Research Center) support program supervised by the NIPA (National IT Industry Promotion Agency) (NIPA-2012-C1090-1200-0002), and by the National Research Foundation of Korea (NRF) grant funded by the Korea Government (MEST) (NRF 2010-0019408).

Notes and references

- J. M. Tarascon and M. Armand, *Nature*, 2001, **414**, 359–367.
- P. G. Bruce, B. Scrosati and J.-M. Tarascon, *Angew. Chem., Int. Ed.*, 2008, **47**, 2930–2946.
- F. Y. Cheng, J. Liang, Z. L. Tao and J. Chen, *Adv. Mater.*, 2011, **23**, 1695–1715.
- B. Dunn, H. Kamath and J. M. Tarascon, *Science*, 2011, **334**, 928–935.
- M. N. Obrovac and L. J. Krause, *J. Electrochem. Soc.*, 2007, **154**, A103–A108.
- S. D. Beattie, D. Larcher, M. Morcrette, B. Simon and J. M. Tarascon, *J. Electrochem. Soc.*, 2008, **155**, A158–A163.
- R. Chandrasekaran, A. Magasinski, G. Yushin and T. F. Fuller, *J. Electrochem. Soc.*, 2010, **157**, A1139–A1151.
- J. R. Szczech and S. Jin, *Energy Environ. Sci.*, 2011, **4**, 56–72.
- L. Y. Beaulieu, K. W. Eberman, R. L. Turner, L. J. Krause and J. R. Dahn, *Electrochem. Solid-State Lett.*, 2001, **4**, A137–A140.
- J. H. Ryu, J. W. Kim, Y. E. Sung and S. M. Oh, *Electrochem. Solid-State Lett.*, 2004, **7**, A306–A309.
- B. Hertzberg, A. Alexeev and G. Yushin, *J. Am. Chem. Soc.*, 2010, **132**, 8548–8549.
- Y. S. Hu, P. Adelhelm, B. M. Smarsly and J. Maier, *ChemSusChem*, 2010, **3**, 231–235.
- N. Liu, H. Wu, M. T. McDowell, Y. Yao, C. Wang and Y. Cui, *Nano Lett.*, 2012, **12**, 3315–3321.
- Y. Park, N.-S. Choi, S. Park, S. H. Woo, S. Sim, B. Y. Jang, S. M. Oh, S. Park, J. Cho and K. T. Lee, *Adv. Energy Mater.*, 2012, **2**, 206–212.
- J. Graetz, C. C. Ahn, R. Yazami and B. Fultz, *Electrochem. Solid-State Lett.*, 2003, **6**, A194–A197.
- A. Magasinski, P. Dixon, B. Hertzberg, A. Kvit, J. Ayala and G. Yushin, *Nat. Mater.*, 2010, **9**, 353–358.
- F. F. Cao, J. W. Deng, S. Xin, H. X. Ji, O. G. Schmidt, L. J. Wan and Y. G. Guo, *Adv. Mater.*, 2011, **23**, 4415–4420.
- K. T. Lee and J. Cho, *Nano Today*, 2011, **6**, 28–41.
- H. Kim, M. Seo, M.-H. Park and J. Cho, *Angew. Chem., Int. Ed.*, 2010, **49**, 2146–2149.
- H. Wu, G. Y. Zheng, N. A. Liu, T. J. Carney, Y. Yang and Y. Cui, *Nano Lett.*, 2012, **12**, 904–909.
- H. Wu, G. Chan, J. W. Choi, I. Ryu, Y. Yao, M. T. McDowell, S. W. Lee, A. Jackson, Y. Yang, L. Hu and Y. Cui, *Nat. Nanotechnol.*, 2012, **7**, 310–315.
- A. M. Chockla, J. T. Harris, V. A. Akhavan, T. D. Bogart, V. C. Holmberg, C. Steinhagen, C. B. Mullins, K. J. Stevenson and B. A. Korgel, *J. Am. Chem. Soc.*, 2011, **133**, 20914–20921.
- P. R. Abel, Y. M. Lin, H. Celio, A. Heller and C. B. Mullins, *ACS Nano*, 2012, **6**, 2506–2516.
- J. Li, R. B. Lewis and J. R. Dahn, *Electrochem. Solid-State Lett.*, 2007, **10**, A17–A20.
- N. S. Choi, K. H. Yew, W. U. Choi and S. S. Kim, *J. Power Sources*, 2008, **177**, 590–594.
- N. S. Hochgatterer, M. R. Schweiger, S. Koller, P. R. Raimann, T. Wöhrle, C. Wurm and M. Winter, *Electrochem. Solid-State Lett.*, 2008, **11**, A76–A80.
- J. Li, L. Christensen, M. N. Obrovac, K. C. Hewitt and J. R. Dahn, *J. Electrochem. Soc.*, 2008, **155**, A234–A238.
- A. Magasinski, B. Zdyrko, I. Kovalenko, B. Hertzberg, R. Burtovyy, C. F. Huebner, T. F. Fuller, I. Luzinov and G. Yushin, *ACS Appl. Mater. Interfaces*, 2010, **2**, 3004–3010.
- I. Kovalenko, B. Zdyrko, A. Magasinski, B. Hertzberg, Z. Milicev, R. Burtovyy, I. Luzinov and G. Yushin, *Science*, 2011, **333**, 75–79.
- G. Liu, S. D. Xun, N. Vukmirovic, X. Y. Song, P. Olalde-Velasco, H. H. Zheng, V. S. Battaglia, L. W. Wang and W. L. Yang, *Adv. Mater.*, 2011, **23**, 4679–4683.
- S. Komaba, N. Yabuuchi, T. Ozeki, Z. J. Han, K. Shimomura, H. Yui, Y. Katayama and T. Miura, *J. Phys. Chem. C*, 2012, **116**, 1380–1389.
- B. Koo, H. Kim, Y. Cho, K. T. Lee, N. S. Choi and J. Cho, *Angew. Chem., Int. Ed.*, 2012, **51**, 8762–8767.
- S. Komaba, K. Shimomura, N. Yabuuchi, T. Ozeki, H. Yui and K. Konno, *J. Phys. Chem. C*, 2011, **115**, 13487–13495.
- S. Y. Yang and M. F. Rubner, *J. Am. Chem. Soc.*, 2002, **124**, 2100–2101.
- M. K. Park, S. X. Deng and R. C. Advincula, *J. Am. Chem. Soc.*, 2004, **126**, 13723–13731.
- A. M. Leahf, M. D. Moussallem and J. B. Schlenoff, *Langmuir*, 2011, **27**, 4756–4763.